Neuron, Vol. 30, 525–536, May, 2001, Copyright ©2001 by Cell Press

Differential Functions of *mPer1*, *mPer2*, and *mPer3* in the SCN Circadian Clock

Kiho Bae,[1,5] Xiaowei Jin,[1,6] Elizabeth S. Maywood,[2] Michael H. Hastings,[2,3] Steven M. Reppert,[1,5] and David R. Weaver[1,4,5]

[1]Laboratory of Developmental Chronobiology
MassGeneral Hospital for Children
Massachusetts General Hospital, and
Harvard Medical School
Boston, Massachusetts 02114
[2]Department of Anatomy
University of Cambridge
Cambridge, CB2 3DY
United Kingdom
[3]Division of Neurobiology
MRC Laboratory of Molecular Biology
Hills Road
Cambridge, CB2 2QH
United Kingdom

Summary

The role of *mPer1* and *mPer2* in regulating circadian rhythms was assessed by disrupting these genes. Mice homozygous for the targeted allele of either *mPer1* or *mPer2* had severely disrupted locomotor activity rhythms during extended exposure to constant darkness. Clock gene RNA rhythms were blunted in the suprachiasmatic nucleus of *mPer2* mutant mice, but not of mPER1-deficient mice. Peak mPER and mCRY1 protein levels were reduced in both lines. Behavioral rhythms of *mPer1*/*mPer3* and *mPer2*/*mPer3* double-mutant mice resembled rhythms of mice with disruption of *mPer1* or *mPer2* alone, respectively, confirming the placement of *mPer3* outside the core circadian clockwork. In contrast, *mPer1*/*mPer2* double-mutant mice were immediately arrhythmic. Thus, mPER1 influences rhythmicity primarily through interaction with other clock proteins, while mPER2 positively regulates rhythmic gene expression, and there is partial compensation between products of these two genes.

Introduction

A circadian clock in the mammalian suprachiasmatic nuclei (SCN) regulates rhythms in physiology and behavior (for reviews, see Weaver, 1998; Klein et al., 1991). SCN neurons contain a cell-autonomous circadian clock (Welsh et al., 1995). The circadian mechanism is thought to be a self-sustaining transcriptional/translational feedback loop in which the expression of putative "clock genes" is suppressed periodically by their protein products (Dunlap,1999; Reppert and Weaver, 2001). An interlocking positive transcriptional loop appears to reinforce and stabilize the negative feedback loop (Shearman et al., 2000b) as in other organisms (Bae et al., 1998; Glossop et al., 1999; Lee et al., 2000).

The negative feedback loop involves the dynamic regulation of three *Period* genes (in the mouse, designated *mPer1–3*) and two Cryptochrome (*mCry1* and *mCry2*) genes. The rhythmic transcription of these genes is driven by the basic helix-loop-helix (bHLH)/PAS-containing transcription factors CLOCK and BMAL1 (Gekakis et al., 1998; Hogenesch et al., 1998; Jin et al., 1999; Kume et al., 1999). At the protein level, the rhythmic abundance of mPER1- and mPER2-immunoreactive nuclei in the SCN is coincident with rhythms in mCRY1 and mCRY2 (Hastings et al., 1999; Kume et al., 1999; Reppert and Weaver, 2001). The synchronization between the timing of the peak levels of these proteins with the decline in their mRNAs is consistent with the proposed autoregulatory mechanism.

The structural homology of the mPERs to the *Drosophila* PERIOD protein, an essential negative element in the fly feedback loop, led to the expectation that the mPERs would function as negative elements in the mammalian feedback loop. In fact, each of the mPERs can modestly inhibit CLOCK:BMAL1-mediated transcription in vitro (Jin et al., 1999; Kume et al., 1999; Sangoram et al., 1998). There is no in vivo evidence to indicate an important role of the mPERs in negative feedback within the clock loop, however. Furthermore, mCRY1 and mCRY2 are potent inhibitors of CLOCK:BMAL1-stimulated transcription (Griffin et al., 1999; Kume et al., 1999), and their activity as negative regulators does not require the PER proteins (Shearman et al., 2000b). In mCRY-deficient mice, *mPer1* and *mPer2* RNA levels are arrhythmic and maintained at moderate to high levels, consistent with *mCry* gene products playing *the* critical role as negative regulators (Okamura et al., 1999; Shearman et al., 2000b; Thresher et al., 1998; van der Horst et al., 1999; Vitaterna et al., 1999).

What then are the function(s) of the mPER proteins? Recent studies suggest that the *mPer* genes have functionally distinct roles. *mPer2* apparently plays a critical role within the core circadian feedback loop, but as a positive factor rather than as a negative regulator, of CLOCK:BMAL1-mediated transcription (Shearman et al., 2000b; Zheng et al., 1999). The importance of mPER2 for behavioral rhythmicity has been demonstrated in both mice and humans. A mutation of the *mPer2* gene resulting in deletion of 87 residues from the protein dimerization PAS domain (*mPer2*^{Brdm1}) leads to circadian instability and delayed arrhythmicity in mice (Zheng et al., 1999). In humans, a mutation in *Per2* that reduces the ability of hPER2 to be phosphorylated by casein kinase Iε is associated with familial advanced sleep phase syndrome, an abnormality in the circadian timing system affecting the timing of sleep (Toh et al., 2001).

In contrast to the robust phenotype of *mPer2*^{Brdm1} mutant mice, mice with targeted disruption of *mPer3* have only a very subtle alteration in circadian rhythmicity consisting of a slight shortening of the cycle length (period) of free-running rhythms in constant conditions (Shearman et al., 2000a). Studies of *mPer1* have focused on its proposed role in entrainment of the SCN by environmental stimuli. *mPer1* and *mPer2* mRNA levels increase in

[4]Correspondence: david.weaver@umassmed.edu
[5]Present address: Department of Neurobiology, University of Massachusetts Medical School, Worcester, MA 01655.
[6]Present address: Biogen Inc., Cambridge, MA 02142.

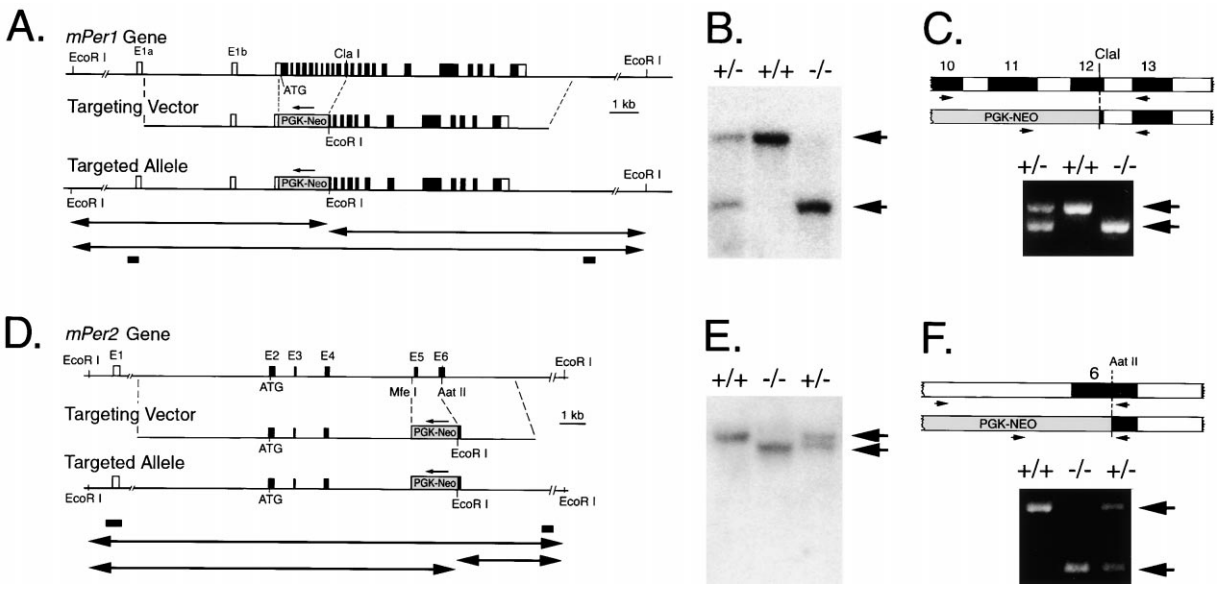

Figure 1. *mPer1* and *mPer2* Targeting Constructs and Genotyping Strategies

(A) Schematic representation of the *mPer1* gene, the targeting construct, and the targeted allele. A 3.0 kb portion of the *mPer1* gene was replaced by a 1.8 kb neomycin resistance cassette (PGK-Neo) in the reverse orientation. Boxes represent exons; lines represent introns. Open boxes represent untranslated regions; filled boxes represent coding region. E1a and E1b represent alternative first exons (Hida et al., 2000). Small bars below the targeted allele indicate the location of probes used for Southern blot analysis.

(B) Genotype determination by Southern blot analysis. An EcoRI site introduced by the neomycin resistance cassette was used to differentiate wild-type and targeted alleles by Southern blotting. DNA from mouse tails was digested with EcoRI and hybridized with the 5′ probe. The EcoRI fragment from the wild-type (+) allele is ~25 kb, and from the targeted (−) allele is ~15 kb.

(C) PCR genotyping strategy and photograph of PCR products amplified from mouse tail DNA. Genotypes are shown above the lanes. Arrows indicate specific bands.

(D) Schematic representation of the *mPer2* gene, the targeting construct, and the targeted allele. A 1.4 kb portion of the *mPer2* gene was replaced by a 1.8 kb neomycin resistance cassette in the reverse orientation.

(E) Southern blot. DNA from mouse tails was digested with EcoRI, and the blot was hybridized with the 5′ flanking probe. The EcoRI fragment from the wild-type (+) allele is ~25 kb, and from the targeted (−) allele is ~19 kb.

(F) Schematic and gel photograph illustrating the PCR method of genotyping $mPer2^{ldc}$ mice. Other conventions as in (C).

the SCN after a nocturnal light pulse that would reset the circadian clock (Albrecht et al., 1997; Shearman et al., 1997; Shigeyoshi et al., 1997; Takumi et al., 1998; Zylka et al., 1998b) and are decreased by stimuli that would produce phase shifts when administered during the day (Horikawa et al., 2000; Maywood et al., 1999). Studies of protein responses in the mouse SCN following light pulses and studies with antisense oligonucleotides also suggest that mPER1, and perhaps mPER2, plays a role in photic entrainment (Akiyama et al., 1999; Field et al., 2000; Wakamatsu et al., 2001).

To examine the importance of mPER1 and mPER2 in circadian rhythmicity, we generated mice with targeted disruption of *mPer1* or *mPer2*. The results indicate that mPER1 and mPER2 have distinct but similarly important roles in circadian clock function. While mPER2 acts as a positive regulator of rhythmic transcription in the SCN, mPER1 apparently influences clock function at a post-transcriptional level, likely through regulating stability of other circadian regulatory proteins via protein-protein interactions. Locomotor behavioral rhythms in mice with targeted disruption of *mPer3* combined with disruption of either *mPer1* or *mPer2* were similar to rhythms in mice with disruption of *mPer1* or *mPer2* alone, indicating that the lack of robust phenotype in mPER3-deficient mice is not due to functional redundancy among members of the *mPer* gene family and confirming the placement of *mPer3* outside the core circadian clockwork.

Results

Generation of Mice with Targeted Disruption of *mPer1*

An *mPer1* targeting construct was generated by replacing genomic DNA containing exons 2–12 of *mPer1* (as defined in GenBank accession number AB030818; Hida et al., 2000) with a neomycin resistance cassette (Figure 1A; see Experimental Procedures). The deleted region begins 96 nucleotides 5′ of the presumed mPER1 translational start site, includes exonic sequence encoding the putative bHLH and PAS domains, and ends in exon 12. Mice homozygous for the *mPer1* targeted allele were viable, fertile, and without gross abnormalities (Figures 1B and 1C). Northern blot analysis with a probe directed to cDNA encoded by exons within the deleted region confirmed the targeting event (data not shown). Furthermore, analysis of mice homozygous for the *mPer1* targeted allele verified the absence of native mPER1 protein (Figure 2); mice homozygous for the targeted allele are thus referred to as "mPER1-deficient mice."

Generation of Mice with Targeted Disruption of *mPer2*

An *mPer2* targeting construct was generated by replacing a portion of genomic DNA containing exon 5 and a portion of exon 6 with a neomycin resistance cassette

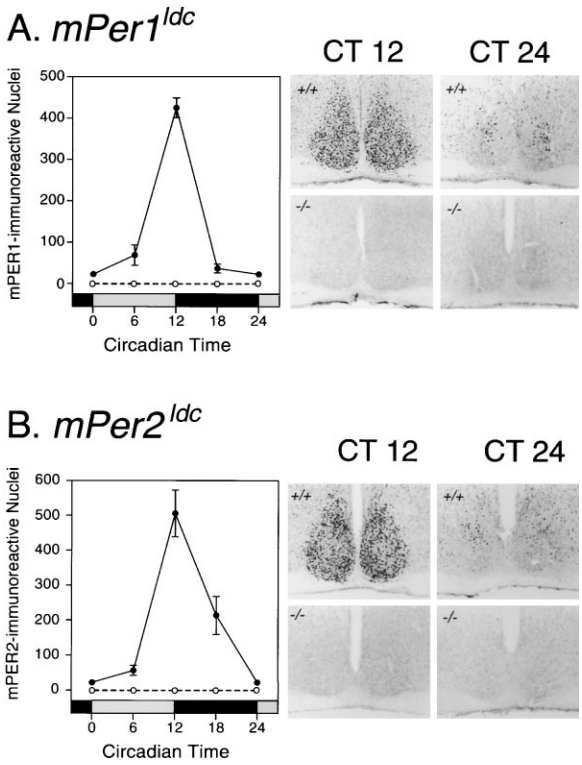

Figure 2. Immunohistochemical Confirmation of Targeted Gene Disruptions

(A) Disruption of *mPer1*. Nuclear mPER1 staining is highly rhythmic in the SCN of wild-type mice (filled circles, solid lines) but is undetectable in the SCN of mPER1-deficient mice (open circles and dashed lines). Values represent mean ± SEM for 3–4 animals per point. Photomicrographs illustrate mPER1 staining in the SCN of wild-type (+/+) and homozygous *mPer1* mutant mice (−/−) at circadian time (CT) 12 and CT 24 on the first day in DD. Bars below the graphs indicate the timing of the prior light-dark cycle.

(B) Disruption of *mPer2*. Nuclear mPER2 staining is highly rhythmic in the SCN of wild-type mice (filled circles, solid lines) but is undetectable in the SCN of homozygous $mPer2^{ldc}$ mutant mice (open circles and dashed lines). Values represent mean ± SEM for 3–4 animals per point. Photomicrographs illustrate mPER2 staining in the SCN of wild-type (+/+) and $mPer2^{ldc}$ mutant mice (−/−) at CT12 and CT 24 on the first day in DD.

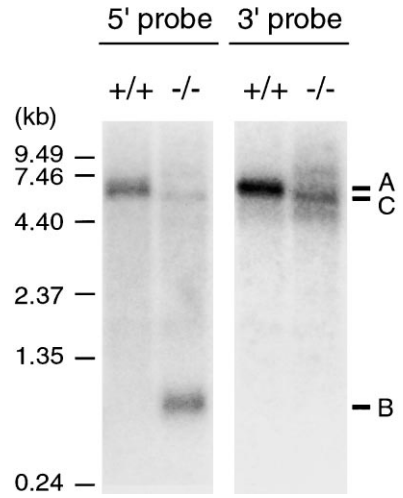

Figure 3. Northern Blot Analysis of Transcripts from the $mPer2^{ldc}$ Targeted Allele

In wild-type mice (+/+), a major transcript band at ~7 kb was detected with probes directed to both the 5′ and 3′ cDNA sequence relative to the site of insertion of the neomycin resistance cassette (band A). In mice homozygous for the targeted allele (−/−), the major transcript identified with the 5′ probe (B) was ~0.8 kb: this transcript also hybridized with a probe based on sequence from intron 4 (data not shown). Minor, long transcripts were also detectable in the homozygous mutant mice with both the 5′ and 3′ probes, likely corresponding to transcripts in which exon 4 is directly spliced to exon 7 (C) as well as transcripts containing a portion of the neomycin cassette between exons 4 and 7. Note that the 3′ probe hybridized more effectively with target mRNA than the 5′ probe; both images were generated from a single blot that was stripped and reprobed. Similar results were obtained in two additional experiments.

(Figure 1D; See Experimental Procedures). Mice homozygous for the *mPer2* targeted allele were viable and fertile, and did not have any gross abnormalities.

Immunohistochemical analysis of the SCN confirmed that mice homozygous for the targeted *mPer2* allele were devoid of detectable mPER2 immunoreactivity (Figure 2). However, RT-PCR and RACE analysis of brain RNA revealed the presence of several *mPer2* transcripts in mice homozygous for the *mPer2* targeted allele (Figure 3 and Experimental Procedures). Several transcript forms, including the major product of the mutant *mPer2* allele, could generate truncated proteins from the first four exons of *mPer2* (Figure 3 and Experimental Procedures). These exons encode the first 147 residues of mPER2; the potential products of these transcripts would lack the entire PAS domain and the remainder of the coding region. A relatively rare transcript form was also detected in which exon 4 was spliced directly to exon 7. This splicing event maintains the reading frame as in native mPER2. This transcript could, if translated, result in a mutant mPER2 protein lacking only the 108 amino acids of the PAS domain encoded by exons 5 and 6 (residues 148–255). The antibody used for assessment of mPER2 immunoreactivity in the SCN is directed to the carboxyl terminus of mPER2, a region that would be present in the deletion mutant protein. The immunohistochemistry data in Figure 2 show that this possible deletion mutant mPER2 protein is not present at detectable levels in the SCN. We conclude that this *mPer2* allele represents a null allele at the level of the SCN.

A previous attempt to disrupt *mPer2* led to mice that express an *mPer2* transcript from which codons for amino acid residues 348–434 were deleted (Zheng et al., 1999). To distinguish the allele and line of mice generated in this laboratory from the $mPer2^{Brdm1}$ mutant mice generated by Zheng et al. (1999), we refer to the allele reported here as $mPer2^{ldc}$.

Circadian Behavior Is Severely Disrupted in Mice with Targeted Disruption of *mPer1* or *mPer2*

Spontaneous locomotor activity was monitored in homozygous mutant and wild-type mice during exposure to a 12 hr light, 12 hr dark lighting cycle (LD), followed by exposure to constant darkness (DD) (Figure 4). In LD, all mice showed higher levels of activity at night, as expected for a nocturnal species. Upon transfer to DD, mice of all genotypes initially showed free-running circadian rhythms. The timing of activity onset in DD was

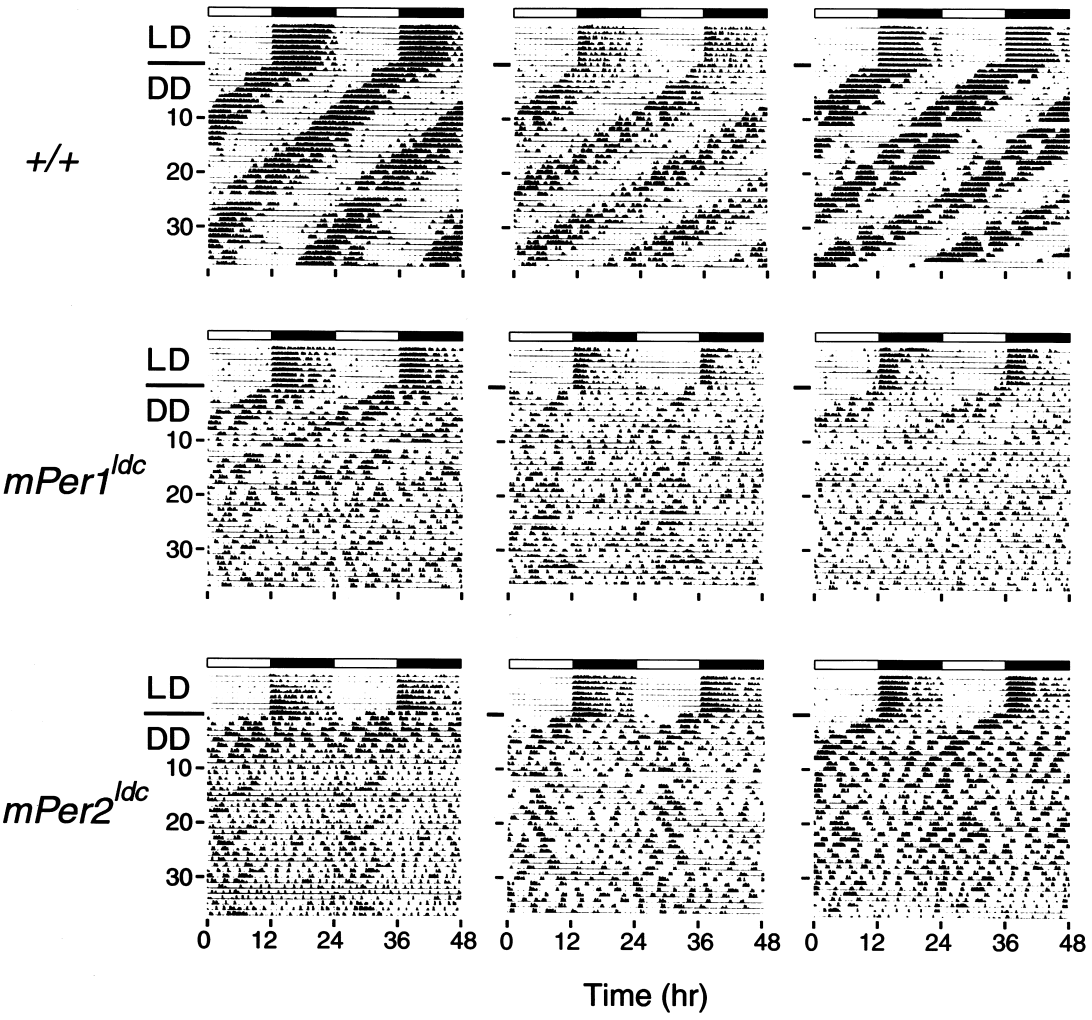

Figure 4. Severe Disruption of Locomotor Activity Rhythms in Mice with Targeted Disruption of *mPer1* or *mPer2*

Activity records (actograms) of representative wild-type mice (+/+; top row), mPER1-deficient (center row), and homozygous *mPer2*^{ldc} mutant (bottom row) mice are shown in double-plotted format. Each horizontal line represents a 48 hr period; the second 24 hr period is plotted to the right and below the first. Vertical bars represent periods of wheel running. Animals were initially housed in a 12L:12D light-dark cycle (LD) and then were transferred to constant darkness (DD). The timing of the light-dark cycle is indicated by the bar above the record. Numbers on the left indicate days in DD. All three wild-type mice shown maintained robust rhythmicity in DD, as did all of the wild-type mice studied. Of the mPER1-deficient mice, the animal on the left maintained weak rhythmicity in DD while the other two animals became arrhythmic by the third 10-day segment in DD. All three *mPer2*^{ldc} mutant mice shown were arrhythmic by the end of the record.

consistent with the phase of activity onset in LD, indicating that all mice had been entrained by the LD cycle. Activity records from representative mice are shown in Figure 4.

Nine of 11 mPER1-deficient mice became arrhythmic following transfer to DD (Figure 4). Most of these mPER1-deficient mice maintained rhythmicity for the first 10–14 days in DD, followed by a severe to total loss of circadian amplitude in the second and third 10-day intervals in DD (see Experimental Procedures; Figure 5). In some cases, very faint rhythmicity was apparent by eye but did not reach the criterion for rhythmicity described in Experimental Procedures (see Figure 4 and supplemental material [http://www.neuron.org/cgi/content/full/30/2/525/DC1]). The transition from rhythmicity to arrhythmicity was gradual and was accompanied by an increase in the amplitude of ultradian components. One mPER1-deficient mouse had markedly reduced amplitude of circadian rhythmicity but with a significant residual component in the circadian range (period = 21.75 hr) for 3 weeks in DD (Figure 4, center row, left panel). Another mPER1-deficient mice maintained robust rhythmicity (period = 24.0 hr) for the duration of study and was not readily distinguishable from wild-type mice (see supplemental material).

All 16 *mPer2*^{ldc} mutant mice examined became arrhythmic following transfer to DD (Figure 4). As with mPER1-deficient mice and *mPer2*^{Brdm1} mutant mice, however, the duration and extent of rhythm persistence in DD was variable. The phenotype of homozygous *mPer2*^{ldc} mutant mice ranged from arrhythmicity upon transfer to DD (Figure 4, bottom row, left panel) to maintenance of rhythmicity for 3 weeks in DD, followed by arrhythmicity. Six mice were arrhythmic within the first 10-day interval and another seven became arrhythmic in the second 10-day interval (e.g., Figure 4, bottom row,

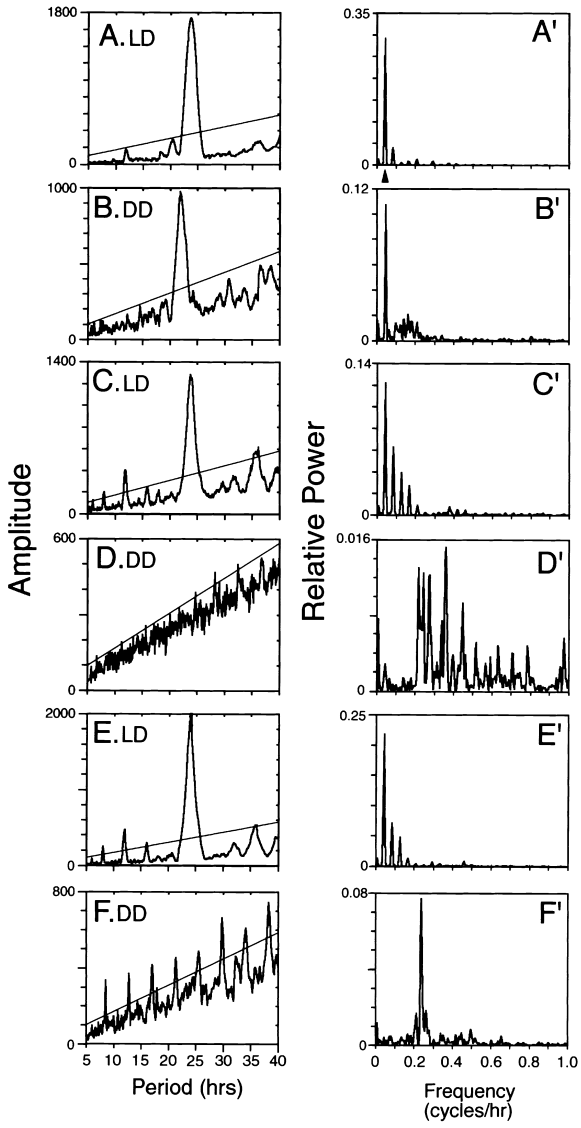

Figure 5. Periodogram (Left) and Fourier Analysis (Right) of Locomotor Activity Rhythms

Plots represent analysis of 10 days of data from representative wild-type (A and B), mPER1-deficient (C and D), and *mPer2*^{ldc} mice (E and F) in LD (A, A′, C, C′, E, and E′) and DD (B, B′, D, D′, F, and F′). Analyses are for the mice whose actograms are shown in the right-hand column of Figure 4. The analyses shown were conducted on the last 10-day segment in LD and on the third 10-day segment in DD of the data shown in Figure 4. A frequency of 0.042 cycles/hr corresponds to 1 cycle/24 hr (indicated by the arrowhead below [A′]). The ascending straight line in the periodograms represents a statistical significance of $p = 0.001$ as determined by the ClockLab program. Note the changes in y axis between panels, indicative of the loss of rhythm amplitude in DD. In LD, all mice had a significant rhythm with a period of 24.0 hr. In the third 10-day interval after release to DD, the mPER1-deficient and *mPer2*^{ldc} mice were arrhythmic. The wild-type mouse maintained rhythmicity in this interval with a period of 21.75 hr.

center panel). All 24 wild-type mice studied in parallel with the mutant animals maintained rhythmicity throughout the study.

The mean free-running period of locomotor activity rhythms upon initial placement in DD did not vary by genotype. The first 2 days after transfer to DD were excluded to allow equilibration to DD, and then the circadian period in the first 10-day interval was calculated. The mean (±SEM) period of mPER1-deficient mice (22.58 ± 0.28 hr, mean ± SEM, n = 11) did not differ significantly from the period of wild-type controls (23.12 ± 0.11, n = 24) or of the 10 *mPer2*^{ldc} mutant mice for which the period could be determined in the initial interval in DD (22.95 ± 0.30 hr; $p > 0.05$, analysis of variance [ANOVA]). As noted above, the period lengths of the two mPER1-deficient mice that maintained rhythmicity in DD were 21.75 and 24.0 hr, spanning the range of values seen in wild-type mice.

Clock Proteins Levels Are Reduced in the SCN of mPER1-Deficient Mice Despite Unaltered Transcript Levels

Examination of clock gene expression and protein levels in the SCN of genetically modified mice has provided important insights into the mechanisms of circadian oscillations (Bunger et al., 2000; Jin et al., 1999; Kume et al., 1999; Shearman et al., 2000a, 2000b; van der Horst et al., 1999). To assess the impact of targeted disruption of *mPer1* on molecular rhythms, patterns of gene expression in the SCN were examined on the first day in DD.

Rhythmic expression of *mPer2*, *mCry1*, and *Bmal1* RNAs was unaltered in the SCN of mPER1-deficient mice (Figure 6). Two-way ANOVA for each gene revealed a significant main effect of time ($p < 0.002$), but no significant effect of genotype and no significant interactions ($p > 0.05$). *mPer1* mRNA was not detectable in mPER1-deficient mice using a probe designed to hybridize with portions of the transcript arising from the deleted genomic region.

In contrast to the lack of effect on SCN gene expression, clock protein rhythms in the SCN were markedly altered in mPER1-deficient mice (Figure 7). In wild-type mice, robust rhythms of nuclear mPER1, mPER2, and mCRY1 were detected on the first day in DD (ANOVA, $p < 0.005$; Figures 2 and 7), consistent with previous reports (Field et al., 2000; Hastings et al., 1999; Kume et al., 1999). mPER1 staining was absent in mPER1-deficient mice (Figure 2). Two-way analysis of variance revealed significant main effects of circadian time and genotype for both mPER2 and mCRY1 ($p < 0.025$). Within each genotype, rhythmicity of mPER2 and mCRY1 was significant (ANOVA, $p < 0.001$). The peak numbers of nuclei immunoreactive for mPER2 and mCRY1 in the SCN of mPER1-deficient mice was reduced by ~50% on the first day in DD, relative to wild-type mice studied in parallel (Figure 7).

Reduced Transcript and Protein Levels in the SCN of *mPer2*^{ldc} Mutant Mice

Gene expression rhythms were markedly altered in *mPer2*^{ldc} mutant mice (Figure 8). In the SCN of mice homozygous for the *mPer2*^{ldc} mutation, *mPer1*, *mCry1* levels were rhythmic, while *mPer2* levels were not. *Bmal1* RNA levels varied significantly with time, but the data from each of two independent experiments were not sinusoidal in shape, e.g., were not rhythmic per se. Two-way analysis of variance revealed a significant main effect of circadian time for each of the four genes, as well as a significant effect of genotype (*mCry1*, *Bmal1*) or a significant interaction (*mPer1*, *mPer2*). Post-hoc,

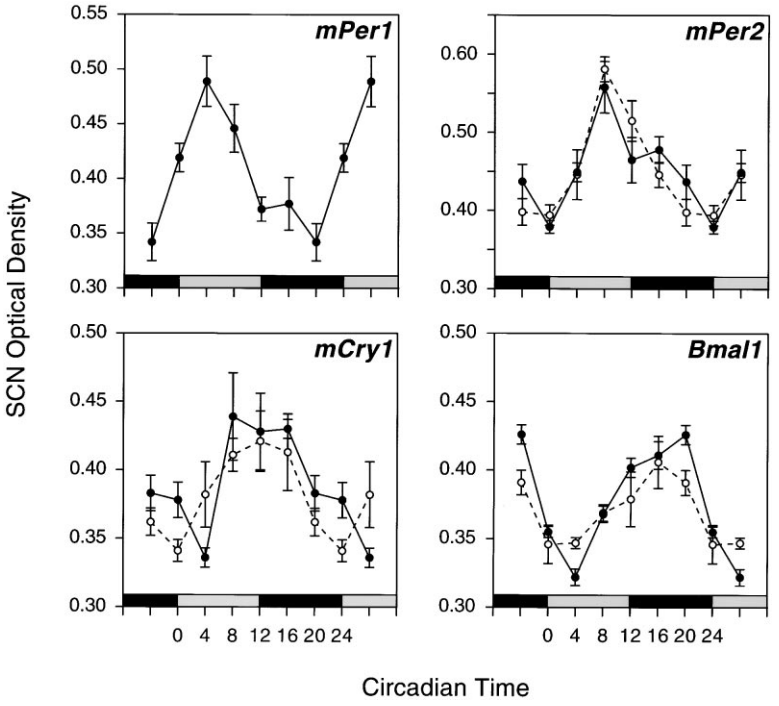

Figure 6. Unaltered Gene Expression Rhythms in the SCN of mPER1-Deficient Mice

Data are presented as the mean ± SEM optical density of the SCN for six to eight mice, measured from film autoradiograms. Filled circles, wild-type mice; open circles, mPER1-deficient mice. Tissues were collected on the first day in DD and were processed for in situ hybridization. *mPer1* transcript was undetectable in mPER1-deficient mice as the probe was directed to exons deleted by the targeting construct. Rhythms of *mPer2*, *mCry1*, and *Bmal1* gene expression were present in both genotypes (ANOVA, $p < 0.001$), and the amplitude of these rhythms did not differ by genotype. The horizontal bar at the bottom of each panel indicates the lighting cycle the animals were exposed to before entry into DD; subjective day is gray and subjective night is black. Circadian times 0 and 12 represent the times the lights would have gone on and off, respectively, had the animals remained in LD. Data from circadian times 20, 24/0, and 4 are double plotted.

pairwise comparisons revealed that mice homozygous for the *mPer2*^{ldc} mutation had significantly depressed peak levels of *mPer1*, *mPer2*, *mCry1*, and *Bmal1* gene expression in the SCN (t tests, $p < 0.05$ for each gene). These results are consistent with previous studies showing reduced levels of gene expression in the SCN of *mPer2*^{Brdm1} mutant mice and further support a role for mPER2 as a positive regulator within the circadian feedback loop (Shearman et al., 2000b; Zheng et al., 1999).

mPER2 immunoreactivity was not detected in the brain of *mPer2*^{ldc} mice (Figure 2). mPER1 and mCRY1 nuclear immunoreactivity remained rhythmic in the mutant mice ($p < 0.05$), but there were marked reductions in the peak level of these antigens in the SCN relative to wild-type controls (Figure 7).

To determine the specificity of the alterations in nuclear mPER1 and mPER2 immunoreactivity in the SCN of mice with targeted *mPer* gene disruptions, we compared *mPer3*-deficient mice with matched wild-type mice on the first day in DD. Numbers of nuclei immunoreactive for mPER1 and mPER2 assessed during the day (circadian time [CT] 2–5) and at night (CT 14–17) were virtually identical in the two genotypes, with both lines having robust rhythms in these antigens (data not shown).

Further Defining the Role of *mPer3*

Previous studies of mice with targeted disruption of *mPer3* revealed only a subtle circadian phenotype (Shearman et al., 2000a), in contrast to the robust phenotype of mice with the mutations in *mPer1* and *mPer2* reported here. One possible explanation for the lack of robust effect of disruption of *mPer3* is that *mPer1* or *mPer2* may be functionally redundant with *mPer3*. Thus, in the presence of functional *mPer1* or *mPer2*, the effect of disrupting *mPer3* may be masked. Precedent for functional redundancy of this sort has been demonstrated between *mCry1* and *mCry2*, where only one allele (from among four) is needed to maintain rhythmicity (van der Horst et al., 1999).

To clarify whether *mPer3* is within the central circadian loop (albeit in a redundant manner), we interbred lines of mice to generate mice homozygous for disruption of both *mPer2* and *mPer3*, as well as mice homozygous for disruption of both *mPer1* and *mPer3*. If there were functional redundancy between *mPer3* and another *mPer* gene, then the phenotype of double-mutant mice should be markedly more severe than the phenotype of the mutations assessed individually. In fact, however, the circadian phenotype of double-mutant mice was no more severe than the phenotype of the more severely affected parental line (Figure 9). These data support the conclusion previously drawn from study of mPER3-deficient mice, that mPER3 does not play an important role in the circadian clock mechanism regulating locomotor activity.

Mice homozygous for mutations of both *mPer1* and *mPer2* were also examined. Each of the four *mPer1*/*mPer2* double-mutant mice showed an abrupt loss of rhythmicity immediately upon transfer to DD (Figure 9). This phenotype is more consistently severe than that seen in the single mutant lines or in any of the other double-mutant lines involving *mPer1*, *mPer2*, and *mPer3*.

Discussion

Previous studies have suggested that mPER1 functions in the input pathway leading to entrainment but have left open the question of whether mPER1 is critical for rhythmicity. The behavioral phenotype of mPER1-deficient mice described here indicates that mPER1 plays an essential role in the maintenance of circadian rhythmicity. This role is distinct from the role played by mPER2. While the behavioral phenotypes of mPER1-

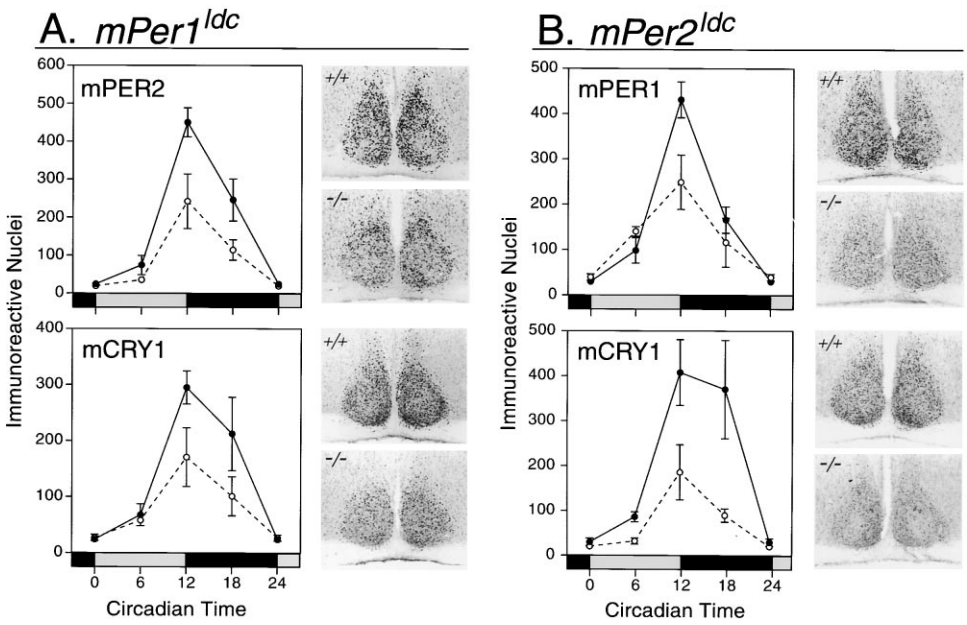

Figure 7. Clock Protein Rhythms Are Altered in Mice with Disruption of *mPer1* or *mPer2*

(A) mPER1-deficient mice. Plots show quantitative assessment of clock proteins in mPER1-deficient mice (open circles and dashed lines) and wild-type mice (filled circles, solid lines). Values represent mean ± SEM for 3–4 animals per point. For each antigen, two-way ANOVA revealed significant effects of genotype and time ($p < 0.05$). Photomicrographs illustrate mPER2 (top) and mCRY1 (bottom) staining in the SCN of wild-type (+/+) and mPER1-deficient mice (−/−) at circadian time 12 on the first day in DD. Bars below the graphs indicate the timing of the prior light-dark cycle. Other plotting conventions as in Figure 2.

(B) *mPer2*^{ldc} mice. Quantitative assessment of clock proteins in homozygous *mPer2*^{ldc} mutant mice (open circles and dashed lines) and in wild-type mice (filled circles and solid lines). Values represent mean ± SEM for 3–4 animals per point. Two-way ANOVA revealed significant effects of genotype and time for mCRY1, and significant effects of time and a significant interaction for mPER1. One-way ANOVAs revealed significant rhythms in the abundance of each antigen in each genotype. Photomicrographs at right illustrate mPER1 (top) and mCRY1 (bottom) staining in the SCN of wild-type (+/+) and *mPer2*^{ldc} mice (−/−) at circadian time 12 on the first day in DD.

deficient and *mPer2*^{ldc} mutant mice were similar, the molecular characteristics of mice bearing these lesions were distinct (Table 1). Disruption of *mPer2* resulted in reduced levels of clock gene expression in the SCN, consistent with the proposed role of mPER2 as a positive regulator of circadian gene expression (Shearman et al., 2000b; Zheng et al., 1999). The reductions in nuclear mPER1 and mCRY1 immunoreactivity in the SCN of *mPer2*^{ldc} mice are likely due to the reductions in peak transcript levels.

Mice homozygous for the targeted *mPer1* allele, in contrast, had unaltered SCN gene expression rhythms but nevertheless had reduced peak numbers of mPER2- and mCRY1-immunoreactive nuclei. The lack of effect of disruption of *mPer1* on *mPer2*, *mCry1*, and *Bmal1* mRNA rhythms may be due to offsetting effects of reductions in mPER2 and mCRY1 protein levels, which play opposite roles in regulating CLOCK:BMAL1-mediated transcription.

Transcriptional assays using cell culture systems indicate that mPER1 can modestly inhibit transcription induced by CLOCK:BMAL1:E-box complexes (Jin et al., 1999; Sangoram et al., 1998). If mPER1 were a major repressor of transcription in vivo, an increase in levels of *mPer2* and *mCry1* RNA levels would be expected in mPER1-deficient mice. This was not observed. Therefore, mPER1 seems unlikely to act as a significant regulator (activator or repressor) of the transcription of these genes in vivo. The reductions in the number of mPER2 and mCRY1 immunoreactive nuclei, occurring despite unaltered levels of the corresponding mRNAs, strongly suggest that mPER1 contributes to the ability of mPER2 and mCRY1 to be detected in the nucleus. A simple interpretation of these data is that mPER1 affects the stability and/or nuclear entry of mPER2 and mCRY1.

Several lines of evidence suggest a role for mPER proteins in interacting with and perhaps stabilizing each other and other clock proteins. First, two-hybrid studies in yeast show that each of the three mPERs can interact with itself, with the other two PERs, as well as with each of the two CRY proteins (Griffin et al., 1999; Zylka et al., 1998a). Second, coimmunoprecipitation experiments demonstrate association of mPER proteins with each other and with the mCRY proteins in the mouse SCN (Field et al., 2000). Third, mCRYs appear to stabilize mPER2 in vivo, as nuclear mPER2 immunoreactivity is markedly reduced in the SCN of *mCry*-deficient mice (Shearman et al., 2000b). Complex protein-protein interactions occur and appear to be important for regulating clock protein stability and/or subcellular localization (Camacho et al., 2001; Keesler et al., 2000; Kume et al., 1999; Lowrey et al., 2000; Vielhaber et al., 2000; Yagita et al., 2000). While the present data focus our attention on a transcriptional role for mPER2 and a posttranscriptional role for mPER1, it is likely that each protein contributes to the circadian feedback loop in several ways.

In all lines of mice studied (including mice with disruption of *mPer1*, *mPer2*, as well as the *mPer1*/*mPer3* and *mPer2*/*mPer3* combinations), the initial phase of activity onset in DD was consistent with the phase of activity

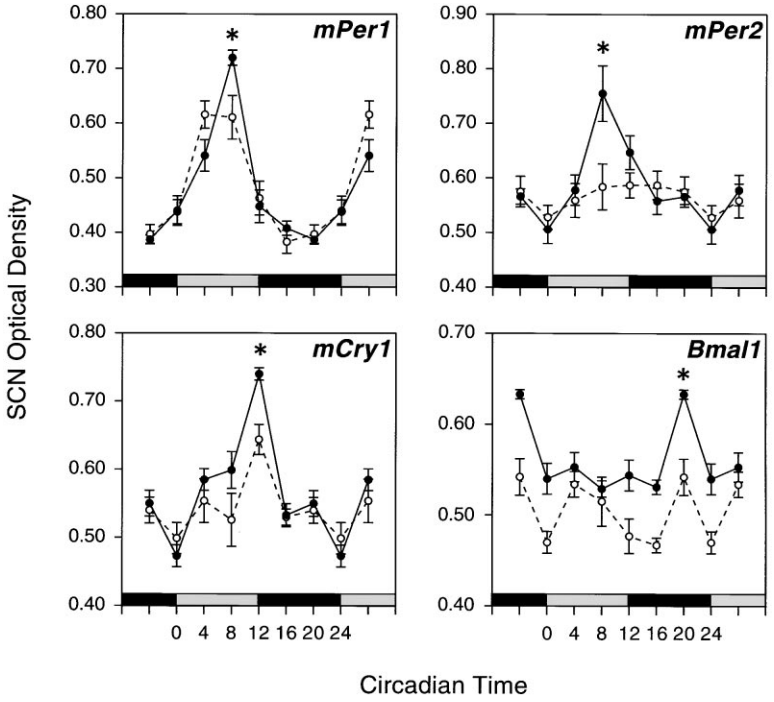

Figure 8. Altered Gene Expression Rhythms in the SCN of *mPer2*^{ldc} Mutant Mice

Data are presented as the mean ± SEM optical density of the SCN for six to eight mice. Filled circles, wild-type mice; open circles, *mPer2*^{ldc} mutant mice. Rhythms of *mPer1*, *mCry1*, and *Bmal1* were present in both genotypes (ANOVA, $p < 0.001$), but the amplitude of rhythmicity was depressed in the *mPer2*^{ldc} mice. Peak levels of gene expression were significantly reduced in homozygous *mPer2*^{ldc} mutant mice (asterisks, $p < 0.05$, t tests). *mPer2* transcripts were detected using a probe to the 5′ region that would detect all transcript forms in the *mPer2*^{ldc} mice. *mPer2* RNA was rhythmic in wild-type mice (ANOVA, $p < 0.0001$) but was not rhythmic in mice homozygous for the mutant allele ($p > 0.05$). Plotting conventions as in Figure 6.

onset in the previous LD cycle. This indicates that the products of these genes are not needed for entrainment to full LD cycles. Albrecht et al. (2001) recently reported that mice lacking mPER1 are deficient in phase advance responses to light, while mice deficient in mPER2 are deficient in phase delays. These results demonstrate that the phase-response curve to light pulses is altered in these mutant lines. This could be due to complete loss of circadian responses to light or to an alteration in the timing or amplitude of response to light.

Studies of mice with genetic alterations of putative clock genes reveal three general phenotypes. The most subtle phenotype is a change in cycle length, as occurs in mCRY1-deficient mice, mCRY2-deficient mice, and mPER3-deficient mice (Shearman et al., 2000a; Thresher et al., 1998; van der Horst et al., 1999; Vitaterna et al., 1999). A second phenotype is gradual loss of rhythmicity with time in DD, with or without period changes. This delayed arrhythmicity phenotype occurs in mice with targeted disruption of *mPer1*, the *mPer2*^{ldc} and *mPer2*^{Brdm1} mutations of mPER2, and the *Clock* mutation (Vitaterna et al., 1994; Zheng et al., 1999; present results). The third phenotype, immediate arrhythmicity, has been described only in mice with targeted disruption of *Bmal1* (MOP3), in *mCry1*$^{-/-}$, *mCry2*$^{-/-}$ double-knockout mice (Bunger et al., 2000; van der Horst et al.,1999; Vitaterna et al., 1999), and in the *mPer1*/*mPer2* double-mutant mice reported here. This array of phenotypes after disruption of "core clock components" suggests that not all clock gene products are equally important for the maintenance of rhythmicity. If each of these clock genes was necessary on a cycle-by-cycle basis, a null mutation in any one of them would presumably result in immediate arrhythmicity. This is not the case, even when those mutations that are not null mutations (e.g., *Clock*; King et al., 1997) are excluded. The observation that some gene products are necessary for the long-term maintenance of rhythmicity but are not needed within each circadian cycle suggests that there is partial redundancy of function among some subsets of clock gene products. Functional redundancy is quite clearly the case with the *mCry* genes: only one wild-type allele from among four (two *mCry1* and two *mCry2* alleles) is needed to maintain rhythmicity (van der Horst et al., 1999).

Our results do not support the hypothesis that *mPer3* is functionally redundant with the other members of the *mPer* gene family. Instead, the current and previous results (Shearman et al., 2000a) strongly suggest that *mPer3* is not essential for the core clock loops. *mPer3* may be involved in regulating circadian outputs other than locomotor activity, or it may literally be "out of the loop." *mPer1* and *mPer2*, in contrast, play important roles in the maintenance of circadian rhythmicity. mPER2 acts as a positive regulator of rhythmic gene expression, while mPER1 apparently influences rhythmicity through interaction with other circadian regulatory proteins. Disruption of either gene destabilizes the circadian system and, in the absence of the priming stimulus of the daily light-dark cycle, leads to severely disrupted rhythmicity with time in constant conditions. Thus, despite the similarity in behavioral phenotype between mice bearing mutations of *mPer1* and *mPer2*, each of the three *mPer* genes has a distinct function in the SCN circadian clockwork.

Experimental Procedures

mPer1 Targeting Construct

Genomic DNA clones were isolated from a 129sv mouse library (Stratagene) using a probe generated from a portion of the *mPer1* cDNA corresponding to nucleotides (nt) 340–761 of GenBank accession number AF022992. The targeting construct was generated in a multistep process. Using PCR, portions of intron 1 and exon 2 were amplified and an XhoI site was introduced into the 3′ end of the amplified product using the primer 5′-AGAAGTCGACGCCTGT CTCTGAGGGCTG-3′. This product was digested with SacII and

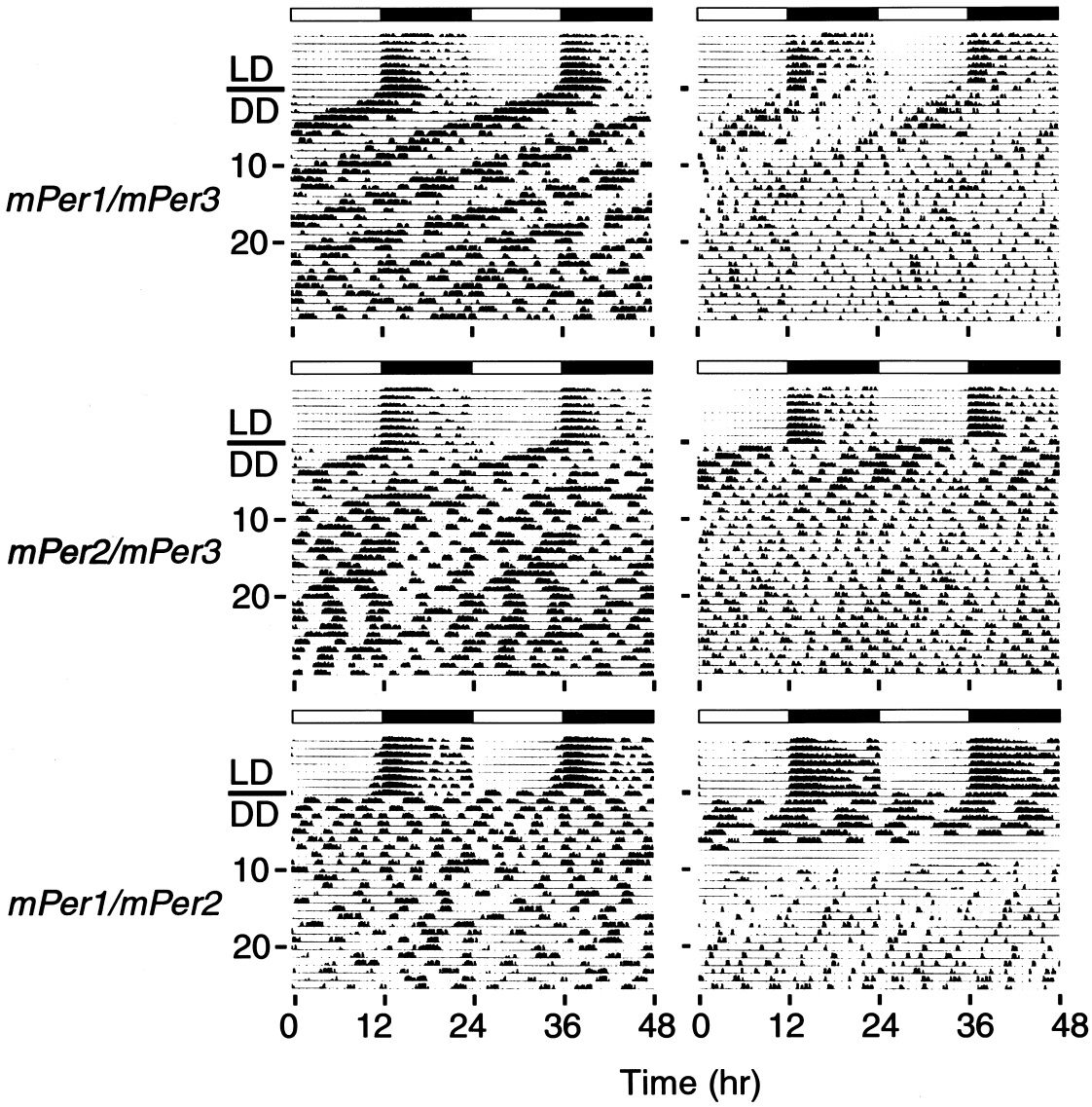

Figure 9. Locomotor Activity Records of Double-Mutant Mice

Mice were entrained to LD then exposed to DD. Top row: actograms of mice homozygous for targeted disruption of both *mPer1* and *mPer3*. Center row: actograms of mice homozygous for targeted disruption of both *mPer2* and *mPer3*. Bottom row: actograms of mice homozygous for targeted disruption of both *mPer1* and *mPer2*. Note the immediate loss of rhythmicity upon transfer to DD in *mPer1/mPer2* double-mutant mice. The *mPer1/mPer3* double-mutant mouse shown in the upper left panel had an initial period in DD of 20.8 hr, the shortest period among the animals of this genotype (group mean 22.02 ± 0.25 hr, n = 7). Sample sizes: *mPer1/mPer3*, n = 7; *mPer2/mPer3*, n = 6; *mPer1/mPer2*, n = 4. Plotting conventions as in Figure 4.

XhoI, and the ~600 bp fragment was ligated to an upstream XhoI-SacII fragment in the vector Bluescript KS, resulting in generation of a 4.5 kb 5′ arm flanked by XhoI sites. The 3′ arm of the construct was generated by digestion of a genomic clone with ClaI, followed by insertion of the neomycin cassette on the 5′ end of the ClaI site. The neomycin resistance cassette consists of the phosphoglycerate kinase promoter driving expression of the neomycin resistance gene (provided by Dr. En Li, Massachusetts General Hospital, Boston). The final construct was assembled by ligation of the 4.5 kb 5′ arm into the vector containing the neomycin resistance cassette and the 9 kb 3′ arm. In the targeting vector, the neomycin construct replaced the genomic region extending from exon 2 (96 bp 5′ of the presumed mPER1 translational start site) through the ClaI site in exon 12. The seams of the construct were sequenced to verify proper assembly of the construct. A partial sequence of the mouse *mPer1* gene has been reported (Hida et al., 2000). Using the numbering in GenBank accession number AB030818, the 5′ arm in the targeting construct corresponds to nt 2106–6665, the deleted region corresponds to nt 6666–9566, and the 3′ end arm is approximately 9 kb in length, extending ~3 kb farther 3′ than the sequence reported in GenBank accession number AB030818.

mPer2 Targeting Construct

A genomic clone was isolated from a 129sv mouse library (Stratagene) using a probe generated from the 5′ region of the *mPer2* cDNA (nt 9–489 of AF035830). A ~10 kb SmaI-MfeI fragment was isolated from the genomic clone and subcloned to Bluescript. This fragment became the 5′ arm of the targeting construct; the MfeI site on its 3′ end is located in intron 4. The 3′ arm, ~3 kb, extended from an AatII site in exon 6 to the 3′ end of the clone. The neomycin resistance cassette was inserted in reverse orientation, replacing ~1.4 kb of genomic DNA, including exon 5 and a portion of exon

Table 1. Behavioral and Molecular Phenotypes of *mPer* Mutant Mice

		mPer1		*mPer2*		*mCry1*		*Bmal1*
Mutation	Behavior	RNA	Protein	RNA	Protein	RNA	Protein	RNA
mPer1^{ldc}	Arrhythmic	absent	absent	no Δ	lower	no Δ	lower	no Δ
mPer2^{ldc}	Arrhythmic	lower	lower	lower	absent	lower	lower	lower
mPer2^{Brdm1}	Arrhythmic[a]	lower[a]	not done	lower[a]	not done	lower[b]	not done	lower[b]
mPer3	Rhythmic[c]	no Δ[c]	no Δ	no Δ[c]	no Δ	no Δ[c]	not done	no Δ[c]

lower, Reduced levels compared to wild-type controls.
no Δ, No change compared to wild-type mice.
[a] Data from Zheng et al., 1999.
[b] Data from Shearman et al., 2000b.
[c] Data from Shearman et al., 2000a.

6 (corresponding to amino acid residues A148–V234 of GenBank number AF035830).

Generation of Mice with Targeted Gene Disruptions

The targeting constructs were linearized with NotI and introduced into embryonic stem (ES) cells by electroporation at the Massachusetts General Hospital Transgenic and Knockout Core Facility. Genomic DNA was extracted from G418/neomycin-resistant ES cell lines, digested with EcoRI, and subjected to agarose gel electrophoresis.

mPer1 ES blots were hybridized with a probe from the 5′ region flanking the *mPer1* targeting cassette (XhoI-XbaI fragment corresponding to nt 1364–2023 of GenBank number AB030818). Candidate positive ES cell lines were confirmed using a 3′ flanking probe. Three positive clones were identified of 196 screened. One positive ES line (#180) used for microinjection generated four chimeric founders, but none gave germline transmission of the targeted allele. A second ES line (#117) was successfully used to generate chimeric founders with germline transmission.

Southern blots of digested ES cell DNA were screened by hybridization with a 3′ probe from the *mPer2* genomic region flanking the targeting construct. One candidate ES cell line (#424) was selected and confirmed using a 5′ flanking probe. This ES line was used for microinjection, generated chimeric founders with germline transmission of the targeted allele.

Chimeric males were bred to isogenic (129/sv) females generously provided by Dr. En Li. F1's receiving the targeted allele were interbred to produce F2 mice homozygous for the targeted allele or homozygous for the wild-type allele. Mice homozygous for the targeted *mPer1* or *mPer2* alleles were viable and fertile, with no gross abnormalities. All studies were conducted using mice of isogenic (129/sv) background.

Genotype Determination

Genotypes were determined by PCR and/or Southern blot analysis of tail biopsy DNA (Figure 1). DNA was digested with EcoRI for Southern blot analysis. Probes for Southern blots were the 5′ and 3′ flanking probes used to identify the ES cell lines radiolabeled with ^{32}P-dCTP (NEN) using random hexamer primers (oligolabeling kit, Boehringer Mannheim). For PCR, amplification reactions were conducted with *Taq* DNA polymerase in Epicentre Technologies PCR buffer E or F. The PCR protocol consisted of 3 min at 94°C, 35 cycles of amplification (each consisting of 30 s at 94°C, 30 s at 60°C, and 90 s at 72°C), and a final extension phase (10 min at 72°C). Products were separated on 1.5% agarose gels containing ethidium bromide and viewed by transillumination.

PCR genotyping for *mPer1* utilized a cocktail of three primers (see Figure 1C). Primers in exons 10 and 13 amplified a band of 773 bp from wild-type genomic DNA. These exonic primers were 5′-CAGTACTTCTCTTTCTACATCCTGAGGACCG-3′, corresponding to nt 8993–9023 of AB030818, and 5′-CATTGCTATCACTGGAGGAGC CAGG-3′, corresponding to the reverse complement of nt 9742–9766 of AB030818. A primer located in the neomycin resistance cassette (Neo 6-2; 5′-TGCCCCAAAGGCCTACCCGCTTCC-3′) and the common reverse primer in exon 13 amplified a ~540 bp band from the targeted allele.

PCR genotyping for *mPer2* utilized a cocktail of three primers (see Figure 1F). A forward primer in intron 5 (xj11; 5′-AGA ACTTGTTGCTCCTGCTT-3′) and a reverse primer in exon 6 (xj8; 5′-GGAAGCTTGTAAGGGGTGGT-3′, corresponding to the reverse complement of nt 842–861 in GenBank number AF035830) amplified a band of ~810 bp from wild-type genomic DNA. A primer located in the neomycin cassette (Neo 6-2, see above) and the common reverse primer in exon 6 amplified a ~400 bp band from the targeted allele.

Identification of Transcripts Expressed from the *mPer2*^{ldc} Targeted Allele

RT-PCR of brain poly (A)$^+$ RNA was performed using the GeneAmp RNA PCR kit (Perkin-Elmer) according to the manufacturer's instruction. The PCR program used was 5 min at 94°C followed by 35 cycles of (45 s at 94°C, 45 s at 60°C, and 90 s at 72°C), and a 10 min extension at 72°C. Forward primers were located in exons 2 (5′-GCTTATTCCAGAGCCCGACATGAATGG-3′, 5′-GACAATGGGAA GGAGCTGCGGATG-3′), 3 (5′-AGCACAACCCCTCCACGAGCGG-3′), and 4 (5′-GGAGTGTGAAGCAGGTGAAGG-3′). The reverse primer was located in exon 10 (5′-GAGTCTTCTCCTCTGGGCACGGGG-3′). RT-PCR with these primer pairs revealed that exon 4 was spliced directly to exon 7 in the mice with the targeted disruption (see below). No other products were detected with these primer pairs. In wild-type mice, the products were consistent with the published cDNA sequence.

3′-RACE was performed using the Marathon cDNA Amplification Kit (Clontech). cDNA was prepared from whole brain of wild-type and *mPer2*^{ldc} mice collected at CT 10. Two gene-specific forward primers were used: 5′-AGCACAACCCCTCCACGAGCGG-3′ (exon 3) and 5′-GCCCTGCGGAGTGTGAAGCAGGTGAAGG-3′ (exon 4). Products were eluted from agarose gels (Qiaex II kit, Qiagen), subcloned into pCRII vector using a TOPO Cloning kit (Invitrogen), and the inserts were sequenced. Primer pairs based on the sequence of RACE products were used in RT-PCR to verify the existence of transcripts identified by RACE.

Northern blot analysis was performed as previously described (Shearman et al., 2000a). Probes for *mPer2* included a probe 5′ of the inserted neomycin cassette (nt 9–489 of AF035830), a probe 3′ of the neomycin cassette (nt 1572–2338 of AF035830), a deletion-specific probe, and a probe to sequence in intron 4.

Several transcript forms were identified that could generate amino-truncated proteins containing the first 147 residues of mPER2. The most abundant forms, as assessed by Northern blot analysis (Figure 3), were two differentially polyadenylated transcripts of ~0.8 kb, in which exon 4 was spliced to a pseudoexon, located between exons 4 and 5. A probe based on the pseudoexon revealed the same ~0.8 kb transcript detected with the 5′ probe. Translation of these transcripts would result in a protein with 151 amino acids, consisting of the first 147 residues of mPER2 plus a 4-residue peptide from the intron. An additional transcript form consisted of exon 4 spliced to a cryptic splice site in the neomycin cassette; translation of this form would result in a protein with 159 amino acids, 12 of which were derived from the translation of cassette sequence before reaching an in-frame stop codon. The size and 3′ terminus of this transcript form were not defined, but it could include exons 3′ of the targeted regions and may be detected by the 3′ probe in Figure 3.

Finally, RACE and RT-PCR detected a transcript form contained exon 4 spliced directly to exon 7; in this transcript, the reading frame was maintained as in native mPER2. This transcript could, if translated, result in a deletion mutant mPER2 protein lacking 108 amino acids encoded by exons 5 and 6 (148–255). Northern blot analysis with a probe directed to the 3′ region of the *mPer2* cDNA revealed that large transcripts were indeed present in mice homozygous for the targeted *mPer2* allele. These larger transcript forms represent a small proportion of the total transcripts containing the 5′ region (Figure 3).

Assessment of Behavioral Rhythms

Animals were housed within light-tight, ventilated environmental compartments in a temperature- and humidity-controlled facility. Except as noted, animals were exposed to a 12L:12D light-dark cycle. Dim red light from fluorescent bulbs was present within each compartment at all times, including those designated as "darkness." For monitoring locomotor activity, male mice were housed individually in cages equipped with running wheels. Magnetic reed switches mounted near the running wheel detected movement of a magnet mounted on the wheel. Switch closures were detected by a computer-based system (DataCol3, MiniMitter, Sunriver, OR) and saved to disk at 5 min intervals. Data were plotted in actogram format using the software within the DataCol package and were double-plotted after scanning into Photoshop 5.0.

Free-running period was estimated from actograms without knowledge of the genotype of the animals. The period was determined from the slope of a hand-drawn line through activity onsets of each animal housed in constant darkness. The first 3–5 days after discontinuation of the lighting cycle were excluded from the analysis to allow stabilization to constant conditions.

To assess persistence of rhythmicity in DD, two methods were used. First, actograms were graded for the presence of rhythmicity by an observer unaware of the genotype of the animals. Actograms were scored as rhythmic (having robust rhythms in DD) or arrhythmic (having a severe to total loss of rhythm amplitude in DD, relative to the behavior of the same mouse in LD). Second, an objective assessment was obtained by exporting the data from the DataCol package using DCSORT and analyzing it using ClockLab (Actimetrics). Ten-day segments of data were analyzed by chi-square periodogram and Fourier transformation (Figure 5). Periodogram analysis assesses the period of rhythmicity in a data set by fitting the data set to candidate periods within a specified range, while Fourier analysis provides a more quantitative assessment of the rhythmicity at the predominant frequency. For these analyses, each animal served as its own control. One segment in LD and two or three consecutive 10-day segments of data in DD (excluding the first 2 days of data after transfer from LD) were assessed. Animals were considered rhythmic when periodogram analysis showed a major and statistically significant ($p < 0.001$) peak in the circadian range, and when the amplitude of rhythmicity of the major peak in the circadian range in DD (assessed by Fourier transform) was at least 20% of the amplitude of the same animal in LD. Conversely, animals termed arrhythmic had a severely dampened amplitude of rhythmicity (amplitude in DD less that 20% the absolute amplitude for the same mouse in LD), and lacked a major, significant peak in the circadian range.

Analysis of SCN Gene Expression

Mice for analysis of gene expression were housed in 12L:12D for at least 10 days prior to analysis. The lighting timer was disabled on the day of study so that the animals remained in constant darkness (DD) on the day of tissue collection. Tissue collection commenced at CT 4 or 6 on the first day in DD and continued until CT 24, where CT 0 is the time of light-on in the previous lighting cycle. Mice were euthanized by carbon dioxide inhalation with the aid of dim red illumination, and then tissues were rapidly dissected and frozen (−80°C).

Gene expression in the SCN was examined by in situ hybridization using methods described previously (Shearman et al., 2000a). Coronal, 15 μm sections through the SCN were hybridized overnight with ^{35}S-labeled complementary RNA probes generated by in vitro transcription (Promega). The templates for probe generation were PCR-generated fragments of cDNAs subcloned into TA vector (Invitrogen). Probes were as follows: *mPer1* (nt 340–761 of accession number AF022992), *mPer2* (nt 9–489 of accession number AF035830), *mCry1* (nt 1081–1793 of accession number AB000777), and *Bmal1* (nt 864–1362 of AF015203). Adjacent sections from the same groups of mice were used for all probes in each study.

Statistical analysis of RNA rhythms was conducted using Statview. Two-way analysis of variance (ANOVA) was used to identify differences between the genotypes, across time, and interaction between these variables. One-way ANOVA was used to verify significant effects of circadian time within each genotype. Genotypes were compared by t tests. For all analyses of gene expression, the significance level was set at $p < 0.05$.

Immunocytochemistry

Assessment of clock proteins was performed as previously described (Hastings et al., 1999; Kume et al., 1999). Mutant and wild-type mice were anesthetized in the dark at CT6, CT12, CT18, and CT24 on the first day in constant darkness. Mice were perfused with 4% paraformaldehyde in 0.1 M phosphate buffer, then brains were removed, postfixed for 3-4 hr, and then transferred to 20% sucrose for cryoprotection. After refrigeration in sucrose for 48–72 hr, brains were frozen and sectioned at 30 μm. Sections were processed in three sets to detect mPER1, mPER2, and mCRY1 immunoreactivity in the SCN of each animal. Results shown in Figures 2 and 7 are from adjacent sets of sections from the same animals.

The mPER1 antisera has been previously described (Hastings et al., 1999). The peptide used to generate this antisera corresponds to amino acid residues 6–21 of mPER1. The mPER2 and mCRY1 antisera were purchased from Alpha Diagnostics, and their validation has been described previously (Field et al., 2000; Hastings et al., 1999; Kume et al., 1999).

Image analysis to measure the number of immunoreactive nuclei per SCN was performed using NIH Image as previously described (Hastings et al., 1999; Kume et al., 1999). Data were analyzed by ANOVA, with the significance level set at $p < 0.05$.

Acknowledgments

This work was supported by NIH grants NS39303 and HD14427 and by the UK Medical Research Council and BBSRC (project 8/S09882). We thank Lauren Shearman, Camala Capodice, Aditi Chavda, Kurtis Gray, and Mark Zylka for assistance, and En Li and Hong Lei for generation of the chimeric founder mice.

Received March 15, 2001; revised May 1, 2001.

References

Akiyama, M., Kouzu, Y., Takahashi, S., Wakamatsu, H., Moriya, T., Maetani, M., Watanabe, S., Tei, H., Sakaki, Y., and Shibata, S. (1999). Inhibition of light- or glutamate-induced *mPer1* expression represses the phase shifts into the mouse circadian locomotor and suprachiasmatic firing rhythms. J. Neurosci. *19*, 1115–1121.

Albrecht, U., Sun, Z.S., Eichele, G., and Lee, C.C. (1997). A differential response of two putative mammalian circadian regulators, *mper1* and *mper2*, to light. Cell *91*, 1055–1064.

Albrecht, U., Zheng, B., Larkin, D., Sun, Z.S., and Lee, C.C. (2001). mPer1 and mPer2 are essential for normal resetting of the circadian clock. J. Biol. Rhythms *16*, 100–104.

Bae, K., Lee, C., Sidote, D., Chuang, K.Y., and Edery, I. (1998). Circadian regulation of a *Drosophila* homolog of the mammalian *Clock* gene: PER and TIM function as positive regulators. Mol. Cell. Biol. *18*, 6142–6151.

Bunger, M.K., Wilsbacher, L.D., Moran, S.M., Clendenin, C., Radcliffe, L.A., Hogenesch, J.B., Simon, M.C., Takahashi, J.S., and Bradfield, C.A. (2000). *Mop3* is an essential component of the master circadian pacemaker in mammals. Cell *103*, 1009–1017.

Camacho, F., Cilio, M., Guo, Y., Virshup, D.M., Patel, K., Khorkova, O., Styren, S., Morse, B., Yao, Z., and Keesler, G.A. (2001). Human casein kinase 1δ phosphorylation of human circadian clock proteins Period 1 and 2. FEBS Lett. *489*, 159–165.

Dunlap, J.C. (1999). Molecular bases for circadian clocks. Cell *96*, 271–290.

Field, M.D., Maywood, E.S., O'Brien, J.A., Weaver, D.R., Reppert, S.M., and Hastings, M.H. (2000). Analysis of clock proteins in mouse SCN demonstrates phylogenetic divergence of the circadian clockwork and resetting mechanisms. Neuron *25*, 437–447.

Gekakis, N., Staknis, D., Nguyen, H.B., Davis, F.C., Wilsbacher, L.D., King, D.P., Takahashi, J.S., and Weitz, C.J. (1998). Role of the CLOCK protein in the mammalian circadian mechanism. Science *280*, 1564–1569.

Glossop, N.R., Lyons, L.C., and Hardin, P.E. (1999). Interlocked feedback loops within the *Drosophila* circadian oscillator. Science *286*, 766–768.

Griffin, E.A., Staknis, D., and Weitz, C.J. (1999). Light-independent role of CRY1 and CRY2 in the mammalian circadian clock. Science *286*, 768–771.

Hastings, M.H., Field, M.D., Maywood, E.S., Weaver, D.R., and Reppert, S.M. (1999). Differential regulation of mPER1 and mTIM proteins in the mouse suprachiasmatic nuclei: new insights into a core clock mechanism. J. Neurosci. *19*, RC11.

Hida, A., Koike, N., Hirose, M., Hattori, M., Sakaki, Y., and Tei, H. (2000). The human and mouse *Period1* genes: five well-conserved E-boxes additively contribute to the enhancement of *mPer1* transcription. Genomics *65*, 224–233.

Hogenesch, J.B., Gu, Y.-Z., Jain, S., and Bradfield, C.A. (1998). The basic helix-loop-helix-PAS orphan MOP3 forms transcriptionally active complexes with circadian and hypoxia factors. Proc. Natl. Acad. Sci. USA *95*, 5474–5479.

Horikawa, K., Yokota, S., Fuji, K., Akiyama, M., Moriya, T., Okamura, H., and Shibata, S. (2000). Nonphotic entrainment by 5-$HT_{1A/7}$ receptor agonists accompanied by reduced *Per1* and *Per2* mRNA levels in the suprachiasmatic nuclei. J. Neurosci. *20*, 5867–5873.

Jin, X., Shearman, L.P., Weaver, D.R., Zylka, M.J., de Vries, G.J., and Reppert, S.M. (1999). A molecular mechanism regulating rhythmic output from the suprachiasmatic circadian clock. Cell *96*, 57–68.

Keesler, G.A., Camacho, F., Guo, Y., Virshup, D., Mondadori, C., and Yau, Z. (2000). Phosphorylation and destabilization of human period 1 clock protein by human casein kinase Iε. NeuroReport *11*, 951–955.

King, D.P., Zhao, Y., Sangoram, A.M., Wilsbacher, L.D., Tanaka, M., Antoch, M.P., Steeves, T.D., Vitaterna, M.H., Kornhauser, J.M., Lowrey, P.L., et al. (1997). Positional cloning of the mouse circadian *Clock* gene. Cell *89*, 641–653.

Klein, D.C., Reppert, S.M., and Moore, R.Y. (1991). Suprachiasmatic Nucleus: The Mind's Clock (New York: Oxford Univerity Press).

Kume, K., Zylka, M.J., Sriram, S., Shearman, L.P., Weaver, D.R., Jin, X., Maywood, E.S., Hastings, M.H., and Reppert, S.M. (1999). mCRY1 and mCRY2 are essential components of the negative limb of the circadian clock feedback loop. Cell *98*, 193–205.

Lee, K., Loros, J.J., and Dunlap, J.C. (2000). Interconnected feedback loops in the *Neurospora* circadian system. Science *289*, 107–110.

Lowrey, P.L., Shimomura, Z., Antoch, M.P., Yamazaki, S., Zemenideds, P.D., Ralph, M.R., Menaker, M., and Takahashi, J.S. (2000). Positional syntenic cloning and functional characterization of a mammalian circadian mutation *tau* . Science *288*, 483–491.

Maywood, E.S., Mrosovsky, N., Field, M.D., and Hastings, M.H. (1999). Rapid down-regulation of mammalian *Period* genes during behavioral resetting of the circadian clock. Proc. Natl. Acad. Sci. USA *96*, 15211–15216.

Okamura, H., Miyake, S., Sumi, Y., Yamaguchi, S., Yasui, A., Muijtjens, M., Hoeijmakers, J.H.J., and van der Horst, G.T.J. (1999). Photic induction of *mPer1* and *mPer2* in *Cry*-deficient mice lacking a biological clock. Science *286*, 2531–2534.

Reppert, S.M., and Weaver, D.R. (2001). Molecular analysis of mammalian circadian rhythms. Annu. Rev. Physiol. *63*, 647–676.

Sangoram, A.M., Saez, L., Antoch, M.P., Gekakis, N., Staknis, D., Whiteley, A., Fruechte, E.M., Vitaterna, M.H., Shimomura, K., King, D.P., et al. (1998). Mammalian circadian autoregulatory loop: a *timeless* ortholog and mPer1 interact and negatively regulate CLOCK-BMAL1-induced transcription. Neuron *21*, 1101–1113.

Shearman, L.P., Zylka, M.J., Weaver, D.R., Kolakowski, L.F., Jr., and Reppert, S.M. (1997). Two *period* homologs: circadian expression and photic regulation in the suprachiasmatic nuclei. Neuron *19*, 1261–1269.

Shearman, L.P., Jin, X., Lee, C., Reppert, S.M., and Weaver, D.R. (2000a). Targeted disruption of the *mPer3* gene: subtle effects on circadian clock function. Mol. Cell. Biol. *20*, 6269–6275.

Shearman, L.P., Sriram, S., Weaver, D.R., Maywood, E.S., Chaves, I., Zheng, B., Kume, K., Lee, C.C., van der Horst, G.T.J., Hastings, M.H., and Reppert, S.M. (2000b). Interacting molecular loops in the mammalian circadian clock. Science *288*, 1013–1019.

Shigeyoshi, Y., Taguchi, K., Yamamoto, S., Takekida, S., Yan, L., Tei, H., Moriya, T., Shibata, S., Loros, J.L., Dunlap, J.C., and Okamura, H. (1997). Light-induced resetting of a mammalian circadian clock is associated with rapid induction of the *mPer1* transcript. Cell *91*, 1043–1053.

Takumi, T., Taguchi, K., Miyake, S., Sakakida, Y., Takashima, N., Matsubara, C., Maebayashi, Y., Okamura, K., Takekida, S., Yamamoto, S., et al. (1998). A light-independent oscillatory gene mPer3 in mouse SCN and OVLT. EMBO J. *17*, 4753–4759.

Thresher, R.J., Vitaterna, M.H., Miyamoto, Y., Kazantsev, A., Hsu, D.S., Petit, C., Selby, C.P., Dawut, L., Smithies, O., Takahashi, J.S., and Sancar, A. (1998). Role of mouse cryptochrome blue-light photoreceptor in circadian photoresponses. Science *282*, 1490–1494.

Toh, K.L., Jones, C.R., He, Y., Eide, E.J., Hinz, W.A., Virshup, D.M., Ptacek, L.J., and Fu Y.-H. (2001). An *hPer2* phosphorylation site mutation in familial advanced sleep phase syndrome. Science *291*,1040–1043. Published online January 11, 2001. Sciencexpress #1057499.

van der Horst, G.T.J., Muijtjens, M., Kobayashi, K., Takano, R., Kanno, S., Takao, M., de Wit, J., Verkerk, A., Eker, A.P., van Leenen, D., et al. (1999). Mammalian Cry1 and Cry2 are essential for maintenance of circadian rhythms. Nature *398*, 627–630.

Vielhaber, E., Eide, E., Rivers, A., Gao, Z.-H., and Virshup, D.M. (2000). Nuclear entry of the circadian regulator mPER1 is controlled by mammalian casein kinase 1ε. Mol. Cell. Biol. *20*, 4888–4899.

Vitaterna, M.H., King, D.P., Chang, A.-M., Kornhauser, J.M., Lowrey, P.L., McDonald, J.D., Dove, W.F., Pinto, L.H., Turek, F.W., and Takahashi, J.S. (1994). Mutagenesis and mapping of a mouse gene, *Clock*, essential for circadian behavior. Science *264*, 719–725.

Vitaterna, M.H., Selby, C.P., Todo, T., Niwa, H., Thompson, C., Fruechte, E.M., Hitomi, K., Thresher, R.J., Ishikawa, T., Miyazaki, J., et al. (1999). Differential regulation of mammalian *period* genes and circadian rhythmicity by cryptochromes 1 and 2. Proc. Natl. Acad. Sci. USA *96*, 12114–12119.

Wakamatsu, H., Takahashi, S., Moriya, T., Inouye, S.T., Okamura, H., Akiyama, M., and Shibata, S. (2001). Additive effect of *mPer1* and *mPer2* antisense oligonucleotides on light-induced phase shift. NeuroReport *12*, 127–131.

Weaver, D.R. (1998). The suprachiasmatic nucleus: a 25-year retrospective. J. Biol. Rhythms *13*, 100–112.

Welsh, D.K., Logothetis, D.E., Meister, M., and Reppert, S.M. (1995). Individual neurons dissociated from rat suprachiasmatic nucleus express independently phased circadian firing rhythms. Neuron *14*, 697–706.

Yagita, K., Yamaguchi, S., Tamanini, F., van der Horst, G.J.T., Hoeijmakers, J.H.J., Yasui, A., Loros, J.J., Dunlap, J.C., and Okamura, H. (2000). Dimerization and nuclear entry of mPER proteins in mammalian cells. Genes Dev. *14*, 1353–1363.

Zheng, B., Larkin, D.W., Albrecht, U., Sun, Z.S., Sage, M., Eichele, G., Lee, C.C., and Bradley, A. (1999). The *mPer2* gene encodes a functional component of the mammalian clock. Nature *400*, 169–173.

Zylka, M.J., Shearman, L.P., Levine, J.D., Jin, X., Weaver, D.R., and Reppert, S.M. (1998a). Molecular analysis of mammalian *Timeless*. Neuron *21*, 1115–1122.

Zylka, M.J., Shearman, L.P., Weaver, D.R., and Reppert, S.M. (1998b). Three *period* homologs in mammals: differential light responses in the suprachiasmatic circadian clock and oscillating transcripts outside of brain. Neuron *20*, 1103–1110.